Supplemental Material (not copyedited or formatted) for: Frank T. Wen, Anup Malani, Sarah Cobey. 2022. "The Potential Beneficial Effects of Vaccination on Antigenically Evolving Pathogens." The American Naturalist 199(2). DOI: https://doi.org/10.1086/717410.

Online Supplement: The potential beneficial effects of vaccination on antigenically evolving pathogens

Frank T. Wen[1,*]

Anup Malani[1,2]

Sarah Cobey[1]

1. The University of Chicago, Department of Ecology and Evolution, Chicago, Illinois 60637;
2. The University of Chicago Law School, Chicago, Illinois 60637;
3. The University of Chicago Pritzker School of Medicine, Chicago, Illinois 60637;

∗ Corresponding author; e-mail: frankwen@uchicago.edu.

1 Supplementary Information

1.1 Vaccination and the invasion fitness of mutants

In the following section, we develop an expectation for how vaccination affects antigenic evolution using a simple determinist model that is not related to the computational model presented in the Results. We use invasion analysis to understand how vaccination affects the invasion fitness of antigenically diverged strains by effectively reducing susceptibility. We develop an expression for the fitness of an invading mutant strain to explain how the antigenic selection gradient changes with vaccination. This preliminary analysis establishes expectations for how vaccines might affect influenza's evolution. Unlike equation-based models, the computational agent-based model allows efficient representation of high-dimensional immune states while allowing open-ended evolution.

Here, S, I, and R represent the fraction of susceptible, infected, and recovered individuals. The birth rate ν and the death rate are equal, so the population size is constant. All individuals are born into the susceptible class. Transmission occurs at rate β, and recovery occurs at rate γ. We vaccinate some fraction p of newborns. In practice, this approximates vaccination of young children, who are primarily responsible for influenza transmission. Vaccinated individuals move into the recovered class.

$$\frac{dS}{dt} = \nu(1-p) - \beta SI - \nu S \tag{S1}$$

$$\frac{dI}{dt} = \beta SI - \gamma I - \nu I \tag{S2}$$

$$\frac{dR}{dt} = \gamma I - \nu R + \nu p \tag{S3}$$

The endemic equilibrium of S_{eq}, I_{eq}, and R_{eq} is

$$S_{\text{eq}} = \frac{\gamma + \nu}{\beta} \equiv \frac{1}{R_0} \tag{S4}$$

$$I_{\text{eq}} = \frac{\nu(R_0(1-p)-1)}{\beta} \tag{S5}$$

$$R_{\text{eq}} = 1 - \frac{1}{R_0} - \frac{\nu(R_0(1-p)-1)}{\beta} \tag{S6}$$

where R_0, the basic reproductive number, is the number of secondary infections from a single infected individual in a totally susceptible population.

The disease-free equilibrium (when $p > 1 - \frac{1}{R_0}$) is

$$S_{[I=0]} = 1 - p \tag{S7}$$

$$I_{[I=0]} = 0 \tag{S8}$$

$$R_{[I=0]} = p \tag{S9}$$

We introduce a single invading mutant $I' = \frac{1}{N}$, where N is the total population size. To find the growth rate of the mutant, we develop an expression for the amount of immunity against the mutant strain. The single mutant has an antigenic phenotype d antigenic units away from the resident. The conversion factor between antigenic units and infection risk is notated by c. Thus, the susceptibility to the mutant is given by $\min\{cd, 1\}$, and immunity to the mutant is $\max\{1 - cd, 0\}$. For convenience of notation, we assume $cd \leq 1$.

We can decompose R_{eq} into immunity conferred by recovery from natural infection R_{n} and immunity conferred by vaccination R_{v}:

$$R_{\text{n}} = 1 - \frac{1}{R_0} - \frac{\nu(R_0 - 1)}{\beta} \tag{S10}$$

$$R_{\text{v}} = \frac{\nu R_0 p}{\beta} \tag{S11}$$

$$R_{\text{eq}} = R_{\text{n}} + R_{\text{v}} \tag{S12}$$

The fraction of the population immune to the invading strain is denoted R'. Assuming that vaccines confer a breadth of immunity relative to natural immunity b,

$$R' = (1 - cd)R_{\text{n}} + (1 - \frac{cd}{b})R_{\text{v}} \tag{S13}$$

Note that when the mutant and resident are identical ($d = 0$), the immunity to the invading strain is identical to the equilibrium immunity, $R' = R_{\text{eq}}$. Allowing for coinfection, the fraction susceptible to the invading strain is

$$S' = 1 - R' - \frac{1}{N} \tag{S14}$$

$$= 1 - R' \tag{S15}$$

for large N. When the vaccination rate exceeds $1 - \frac{1}{R_0}$, the resident is eradicated and S' and R'

are calculated using the disease-free equilibrium.

The invasion fitness s of the mutant relative to the endemic strain is the difference between the per-capita growth rates. Note that since the resident is in equilibrium, $dI/dt = 0$.

$$s = \frac{1}{I'}\frac{dI'}{dt} - \frac{1}{I}\frac{dI}{dt} = [\beta S' - (\gamma + \nu)] - 0 \tag{S16}$$

$$= \beta S' - (\gamma + \nu) \tag{S17}$$

The value of s increases with greater distance between the mutant and resident, but decreases as more hosts become vaccinated (Fig. S1A). The expected s can be used to determine the effect of the vaccination fraction p on the expected invasion fitness of the mutant, $\frac{\partial \mathbf{E}(s)}{\partial p}$. $\mathbf{E}(s)$ is a function of the expected distance of a mutant $\mathbf{E}(d)$. In our model, we assume gamma-distributed mutation sizes with a mean δ_{mean} of 0.3 antigenic units and standard deviation δ_{sd} of 0.6 antigenic units (Fig. S1C).

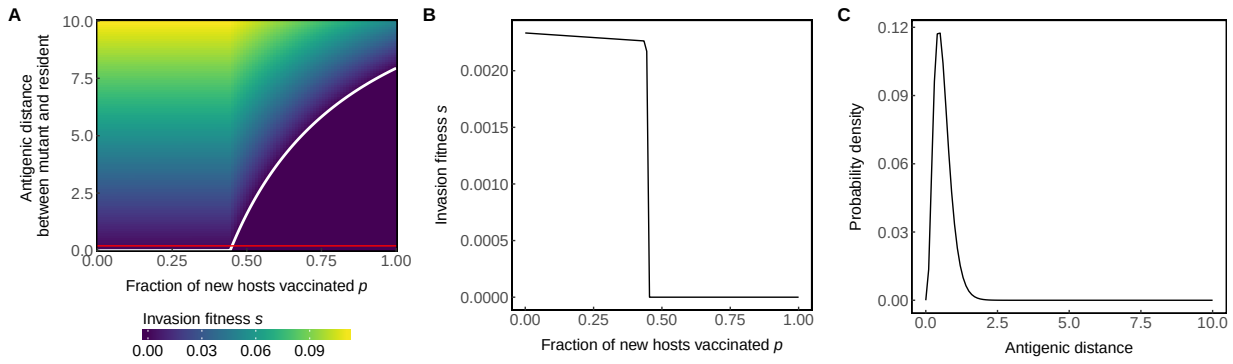

Figure S1: (A) High vaccination rates decrease the invasion fitness of mutant strains. For a given vaccination rate, the invasion fitness of a mutant increases with antigenic distance. However, the invasion fitness of a mutant at a given distance decreases as vaccination coverage increases. An example profile of invasion fitnesses is shown for $d = 0.2$ (the red line) in (B). Above the invasion threshold for the resident ($\rho > 1 - 1/R_0$), the mutant must be increasingly more distant to invade. The white curve shows the invasion threshold, where the invasion fitness for the mutant strain is zero. Mutants above the above the curve can invade, while mutants below the curve cannot. (C) Density of gamma-distributed mutations with a $\delta_{\text{mean}} = 0.3$ and $\delta_{\text{sd}} = 0.6$.

We decompose $\frac{\partial \mathbf{E}(s)}{\partial p}$ to understand how vaccines affect selection by changing susceptibility:

$$\frac{\partial \mathbf{E}(s)}{\partial p} = \left(\frac{\partial \mathbf{E}(s)}{\partial S'}\right)\left(\frac{\partial S'}{\partial R'}\right)\left(\frac{\partial R'}{\partial R_{\mathrm{v}}}\right)\left(\frac{\partial R_{\mathrm{v}}}{\partial p}\right) \tag{S18}$$

$$= (\beta)(-1)(1 - \frac{c\mathbf{E}(d)}{b})(\frac{\nu R_0}{\beta}) \tag{S19}$$

Since $1 - \frac{c\mathbf{E}(d)}{b} \geq 0$ (i.e., one cannot be more than 100% immune to infection), vaccination must decrease the expected invasion fitness of the mutant, $\frac{\partial \mathbf{E}(s)}{\partial p} \leq 0$, slowing evolution. This decrease is attributed to vaccination reducing susceptibility to the mutant by increasing immunity ($\frac{\partial S'}{\partial R'} \leq 0$ and $\frac{\partial R'}{\partial p} > 0$) against any mutant. A larger breadth of vaccine-induced immunity (b) also decreases the expected invasion fitness.

1.2 Model validation without antigenic evolution

In the main text, we show general agreement between our simulations and observations of influenza's epidemiology and evolution using our parameterization. We further validate the epidemiological processes of our agent-based model by removing evolution and comparing output against analytic solutions to a model using deterministic ordinary differential equations. A simple analytic solution to a model with antigenic evolution is intractable. Without vaccination, we find agreement between the simulated equilibrium fraction susceptible and the theoretical S^* for a range of influenza-like values of R_0 (1.2-3.0) (Fig. S2).

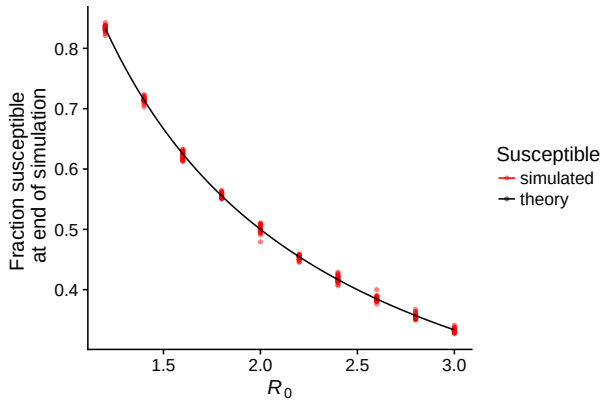

Figure S2: Simulated susceptible fraction at the end of 20 years without vaccination. The theoretical equilibrium fraction susceptible is given by $S^* = \frac{1}{R_0}$. There are 40 replicate simulations shown for each value of R_0.

With vaccination, we validate the model with the probability of revaccination set 100%. In this scenario, a constant fraction of the population is selected for vaccination each year and the same hosts are vaccinated every year. Classical SIR models typically model vaccination of newborns only (Anderson and May 1992). The equilibrium dynamics of a newborn-only vaccination model is the same as the equilibrium dynamics of the complete revaccination model, since at equilibrium, the fraction of vaccinated hosts is equal to the vaccination coverage. The newborn-only vaccination model is given by

$$\frac{dS}{dt} = \nu(1-p) - \beta SI - \nu S \tag{S20}$$
$$\frac{dI}{dt} = \beta SI - \gamma I - \nu I \tag{S21}$$
$$\frac{dR}{dt} = \gamma I - \nu R \tag{S22}$$
$$\frac{dV}{dt} = p - \nu V \tag{S23}$$

Here, the threshold eradication coverage is given by

$$p_t = 1 - 1/R_0 \equiv \frac{\gamma + \nu}{\beta}. \tag{S24}$$

Again, we find agreement between the simulated and theoretical eradication threshold vacci-

nation coverages over a range of influenza-like values of R_0 (Figs. S3, S4). Because we initialize the simulations at the endemic equilibrium *without* vaccination, some damped oscillation is to be expected, which may cause eradication at slightly lower vaccination rates than expected by theory (Fig. S5). For instance, at $R_0 = 1.8$, theory predicts eradication at $p = 0.44$, while simulation achieves extinction in 20/20 simulations within 20 years at $p = 0.42$ (Fig. S5).

The expected period of damped oscillation is derived from stability analysis. The Jacobian matrix of the $SIRV$ model is given by

$$\mathbf{J} = \begin{pmatrix} -\beta I^* - \nu & -\beta S^* & 0 & 0 \\ \beta I^* & \beta S^* - \gamma - \nu & 0 & 0 \\ 0 & \gamma & -\nu & 0 \\ 0 & 0 & 0 & -\nu \end{pmatrix} \tag{S25}$$

where S^* and I^* are the equilibrium fraction susceptible and infected, respectively. The period of oscillation (T) is inversely proportional to the imaginary part of the dominant eigenvalue of the Jacobian matrix (Λ).

$$T = 2\pi / \mathrm{Im}(\Lambda) \tag{S26}$$

$$= 2\pi / \left[-\frac{\gamma^2 + \beta^2 (I^* - S^*)^2 - 2\beta\gamma(I^* + S^*)}{4} \right]^{\frac{1}{2}} \tag{S27}$$

The timeseries (Fig. S5) show oscillation at annual vaccination coverages of 36% and 40%. The calculated periods of oscillations at these rates are 10.3 years and 14.2 years respectively, which roughly agree with the timeseries. Since the simulation has stochastic components, the periodicity appears more regular at first and becomes less predictable over time.

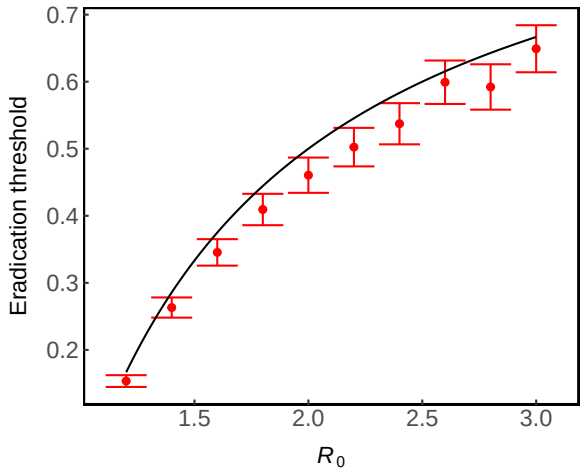

Figure S3: With vaccination, the simulated eradication thresholds agree with analytic predictions. The simulated threshold is the minimum vaccination coverage where 20/20 simulations go extinct within 10 years. Error bars show the sampling resolution (Fig. S4). Simulations were initialized at the analytically derived equilibrium S, I, and R with vaccination (equation S24). There are 20 replicate simulations shown for each value of R_0.

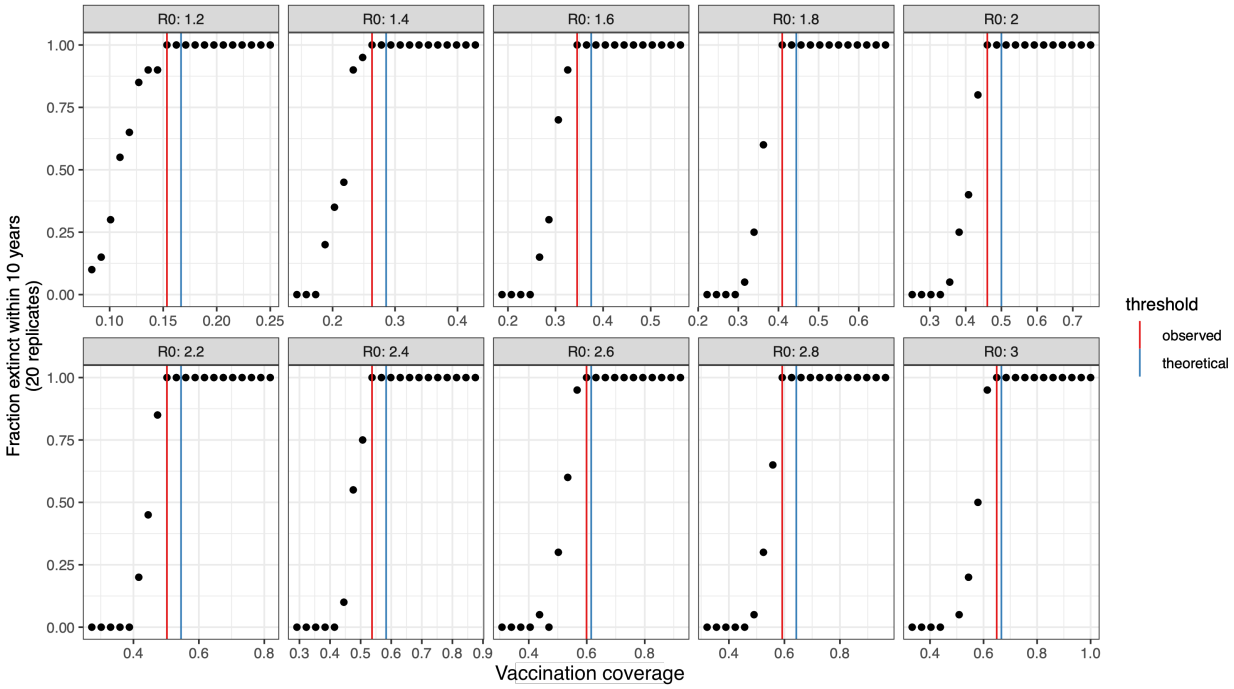

Figure S4: Estimation of simulated eradication thresholds without evolution, starting at the equilibrium S, I, and R with vaccination. To generate response curves, we ran 20 replicate simulations for each combination of R_0 and vaccination coverage and calculated the fraction of extinct simulations. The simulated eradication threshold is the minimum vaccination coverage that causes 20/20 simulations to go extinct within 10 years. When the analytic equilibrium I was nonnegative, we initialized the simulation with a single infection.

Supplemental Material (not copyedited or formatted) for: Frank T. Wen, Anup Malani, Sarah Cobey. 2022. "The Potential Beneficial Effects of Vaccination on Antigenically Evolving Pathogens." The American Naturalist 199(2). DOI: https://doi.org/10.1086/717410.

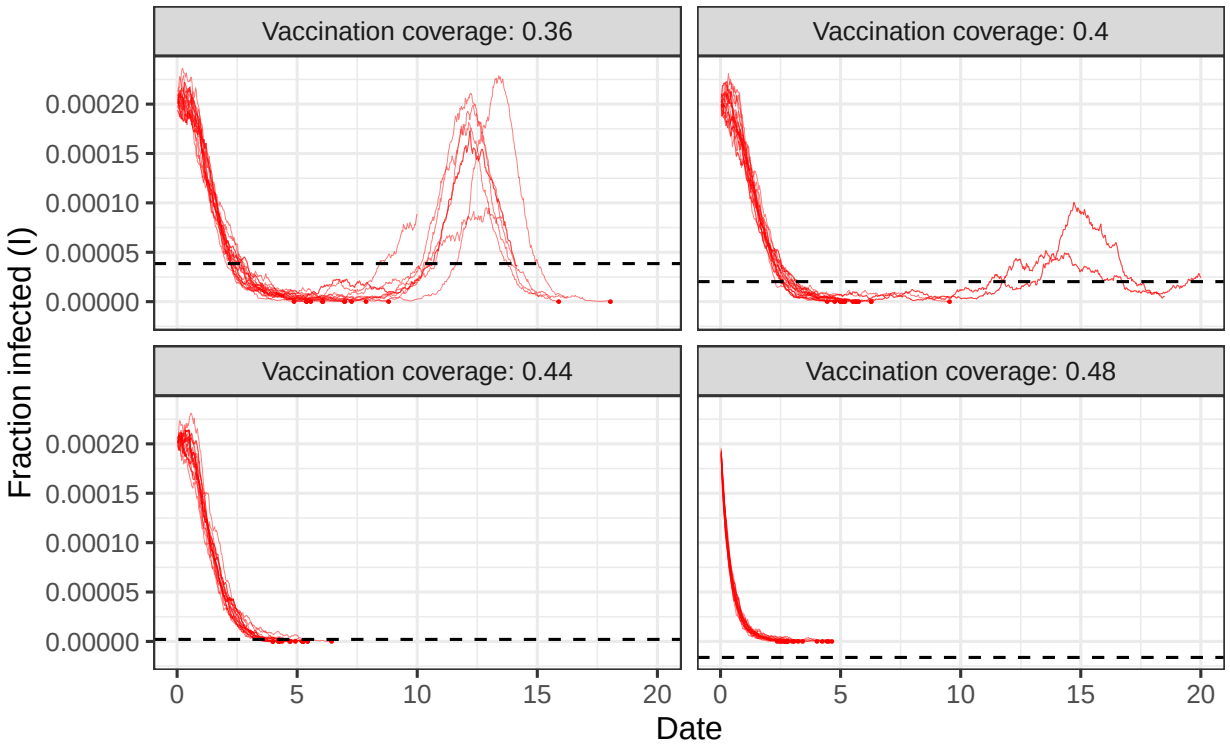

Figure S5: Simulated timeseries without evolution, starting at the endemic equilibrium *without* vaccination, as in the manuscript, but in contrast to Appendix Figures 2 and 3). Here $R_0 = 1.8$, which yields an expected eradication vaccination coverage of 0.44. Because the population starts away from the vaccinated equilibrium, the system experiences damped oscillations, which increase the probability of stochastic extinction. Thus, we observe extinction even when the vaccination coverage is slightly below the expected eradication threshold. Vaccination remains pulsed in 9-month periods, as in the model. Frequencies of susceptible infected (I) individuals are shown for 20 replicate simulations. The dashed lines shows the expected equilibrium frequencies of infecteds. Red points indicate extinction events.

2 Supplementary methods

2.1 Vaccination with repeat vaccination probability and a never-vaccinated population

The main results use a model where, for every season, vaccinated hosts have an 80% probability of being vaccinated in the next season. In addition, 33% of the population is never vaccinated. In the first season, a fraction of hosts (equal to the specified annual vaccination coverage) are randomly selected as candidates for vaccination. During the season, hosts are vaccinated at a Poisson rate r_{day} (Equation 2) such that all of the candidate hosts are expected to be vaccinated at the end of the season. At the end of the season, 20% of hosts who were vaccinated are randomly replaced with hosts who were not vaccinated during that season and are not non-recipients. This establishes the new pool of candidates for vaccination for the next season. In this pool, 80% of hosts were vaccinated in the current season and 20% were not, and fraction of the total population in the candidate host pool is expected to be equal to the annual vaccination coverage. This process repeats until the end of the simulation. In order to initialize the simulation near equilibrium, candidates for vaccination are initially selected from hosts that have immunity to the initial strain. If there are more candidate hosts than immune hosts, then susceptible hosts are also added to the pool of candidates to meet the specified vaccination coverage.

2.2 Totally random vaccination

We tested an alternative version of our model where vaccine recipients are selected at random each year from the entire population (i.e. vaccination is implemented as a vaccination rate instead of as vaccination coverage). In this implementation of vaccination, Vaccine recipients are selected at random each day with replacement, so the total fraction of individuals vaccinated at the end of a vaccine season is slightly less than the annual vaccination rate. For example, at a 5% annual vaccination rate, approximately 4.9% of individuals in the population are vaccinated every year. Since individuals are randomly vaccinated each year, the fraction of ever-vaccinated

individuals increases from one season to the next. For example, at a 5% annual vaccination rate, ∼48.4% of the population has been vaccinated at least once by the twentieth year Note that this cumulative vaccination coverage reflects accumulation of vaccinated individuals and loss of vaccinated individuals due to population turnover. At this rate, vaccination effectively renders 26.0% of individuals immune when vaccination is in equilibrium with antigenic evolution.

Literature Cited

Anderson, R. M., and R. M. May. 1992. Infectious Diseases of Humans: Dynamics and Control. OUP Oxford.

Arevalo, P., H. Q. McLean, E. A. Belongia, and S. Cobey. 2020. Earliest infections predict the age distribution of seasonal influenza A cases. eLife 9:e50060. Publisher: eLife Sciences Publications, Ltd.

Bedford, T., A. Rambaut, and M. Pascual. 2012. Canalization of the evolutionary trajectory of the human influenza virus. BMC Biology 10:38.

Biggerstaff, M., S. Cauchemez, C. Reed, M. Gambhir, and L. Finelli. 2014. Estimates of the reproduction number for seasonal, pandemic, and zoonotic influenza: a systematic review of the literature. BMC Infectious Diseases 14:1–20.

Carrat, F., E. Vergu, N. M. Ferguson, M. Lemaitre, S. Cauchemez, S. Leach, and A.-J. Valleron. 2008. Time lines of infection and disease in human influenza: a review of volunteer challenge studies. American Journal of Epidemiology 167:775–785.

Gupta, V., D. J. Earl, and M. W. Deem. 2006. Quantifying influenza vaccine efficacy and antigenic distance. Vaccine 24:3881–3888.

Jackson, C., E. Vynnycky, and P. Mangtani. 2010. Estimates of the transmissibility of the 1968 (Hong Kong) influenza pandemic: evidence of increased transmissibility between successive waves. American Journal of Epidemiology 171:465–478.

Kwong, J. C., H. Chung, J. K. Jung, S. A. Buchan, A. Campigotto, M. A. Campitelli, N. S. Crowcroft, J. B. Gubbay, T. Karnauchow, K. Katz, A. J. McGeer, J. D. McNally, D. C. Richardson, S. E. Richardson, L. C. Rosella, K. L. Schwartz, A. Simor, M. Smieja, and G. Zahariadis. 2020. The impact of repeated vaccination using 10-year vaccination history on protection against influenza in older adults: A test-negative design study across the 2010/11 to 2015/16 influenza seasons in Ontario, Canada. Eurosurveillance 25.

Lindley, M. C., A. Srivastav, M. Hendrich, H. Fisun, K. Nguyen, O. Pedraza, H. Razzaghi, J. A. Singleton, and W. W. Williams. 2020. Early-Season Influenza Vaccination Uptake and Intent Among Adults – United States, September 2020.

McLean, H. Q., M. G. Thompson, M. E. Sundaram, J. K. Meece, D. L. McClure, T. C. Friedrich, and E. A. Belongia. 2014. Impact of Repeated Vaccination on Vaccine Effectiveness Against Influenza A(H3N2) and B During 8 Seasons. Clinical Infectious Diseases 59:1375–1385.

Park, A. W., J. M. Daly, N. S. Lewis, D. J. Smith, J. L. N. Wood, and B. T. Grenfell. 2009. Quantifying the impact of immune escape on transmission dynamics of influenza. Science 326:726–728.

UN. 2013. World Population Prospects: The 2012 Revision. United Nations, Department of Economic and Social Affairs, Population Division, New York.

Uscher-Pines, L., A. Mulcahy, J. Maurer, and K. Harris. 2014. The Relationship between Influenza Vaccination Habits and Location of Vaccination. PLOS ONE 9:e114863. Publisher: Public Library of Science.

3 Supplementary tables and figures

Table S1: Default parameters

Parameter	Value	Reference
Intrinsic reproductive number (R_0)	1.8	(Biggerstaff et al. 2014; Jackson et al. 2010)
Duration of infection $1/\gamma$	5 days	(Carrat et al. 2008)
Population size N	50 million	(see text)
Birth/death (turnover) rate ν	$1/30$ year^{-1}	(UN 2013)
Mutation rate μ	10^{-4} day^{-1}	(see text)
Mean mutation step size δ_{mean}	0.6 antigenic units	(see text)
SD mutation step size δ_{sd}	0.3 antigenic units	(see text)
Infection risk conversion c	0.07	(Bedford et al. 2012; Gupta et al. 2006; Park et al. 2009)
Duration of simulation	20 years	
Annual vaccination coverage r	0.0-0.5	
Breadth of vaccine-induced immunity b	100%	
Temporal lag between vaccine strain selection and distribution θ	300 days	
Fraction of hosts vaccinated in the current season who are also vaccinated in the next season	0.8	(Arevalo et al. 2020; Kwong et al. 2020; Lindley et al. 2020; McLean et al. 2014; Uscher-Pines et al. 2014).
Fraction of hosts who are never vaccinated	0.33	(Arevalo et al. 2020; McLean et al. 2014; Uscher-Pines et al. 2014).

Table S2: Sample panel data. Each row represents data for for individual i in simulation j at time τ. I is an indicator for infection status (1 if infected and 0 if not), and V is an indicator for vaccination status (1 if vaccinated 0 if not). r_1 is an indicator for 1% vaccination coverage, r_5 for 5%, and r_{10} for 10%.

Identifier			Data								Interpretation
τ	i	j	$I_{ij\tau}$	$V_{ij\tau-1}$	$V_{ij\tau-2}$	$V_{ij\tau-3}$	$V_{ij\tau-4}$	R_{1ij}	R_{5ij}	R_{10ij}	
1	1	1	1	0	1	0	0	0	1	0	The host was infected this season (1) and only vaccinated 2 seasons ago. The population vaccination coverage is 5%
1	2	1	0	1	0	0	1	0	1	0	Host not infected this season (1). Host vaccinated this season and 4 seasons ago. Population vaccination coverage is 5%
...											
10	1	2	1	0	0	0	1	0	0	1	Host infected this season (10). Host vaccinated 4 seasons ago. Population vaccination coverage is 10%

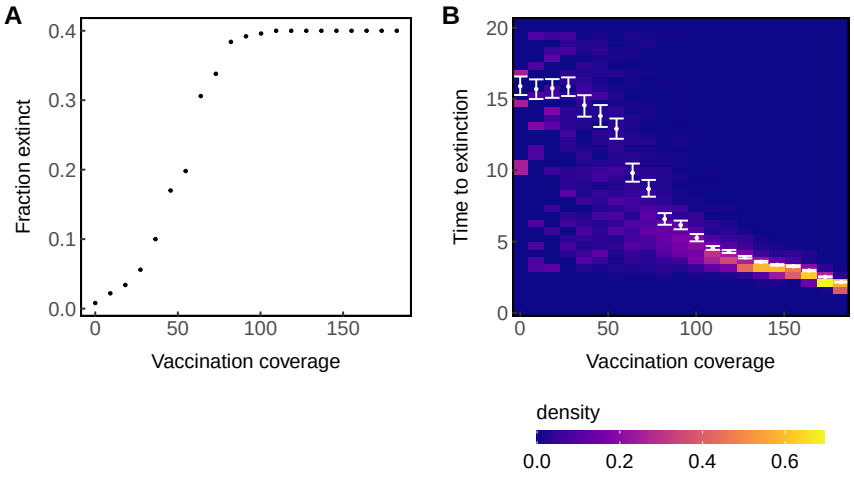

Figure S6: High vaccination coverage increase the probability of extinction and shorten the average time to extinction. (A) Points show the fraction of simulations where the viral population went extinct before 20 years. (B) Density of times to extinction. Points show mean cumulative antigenic evolution or incidence for each vaccination coverage. Error bars show 95% nonparametric bootstrapped confidence intervals of the mean. Data are collected from 500 total simulations for each vaccination coverage with excessively diverse simulations (TMRCA $>$ 10 years) excluded, leaving $\sim$250-400 simulations per rate.

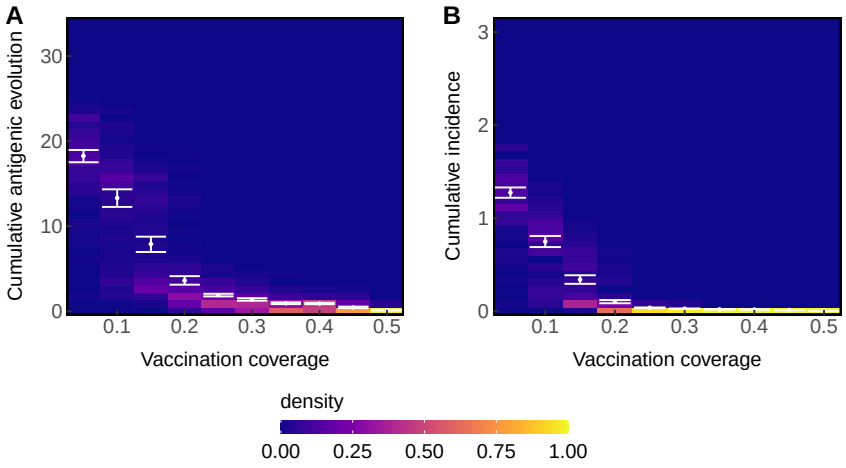

Figure S7: With no temporal lag between vaccine strain selection and distribution, increasing the vaccination coverage quickly decreases the average amount of (A) cumulative antigenic evolution (A) and (B) incidence. Points show mean cumulative antigenic evolution or incidence for each vaccination coverage. Error bars show 95% nonparametric bootstrapped confidence intervals of the mean. Data are collected from 200 total simulations for each vaccination coverage with excessively diverse simulations (TMRCA $>$ 10 years) excluded, leaving $\sim$100-180 simulations per rate.

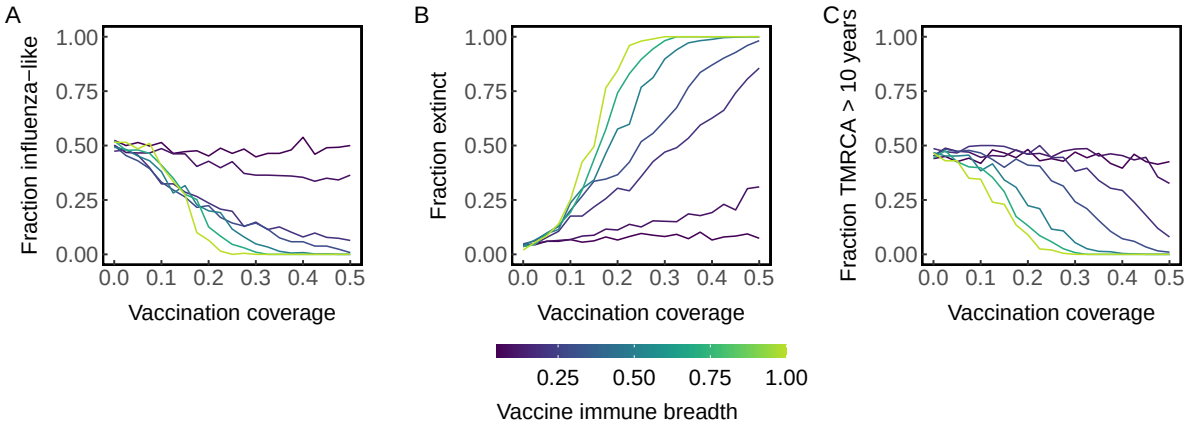

Figure S8: Increasing the vaccination coverage increases the probability that the viral population will go extinct (B) and decreases the probability of exhibiting influenza-like dynamics (endemicity and low diversity) (A) or excessive diversification (TMRCA $>$ 10 years) (C). Lines are colored according to the breadth of the vaccine. Data are collected from 500 replicate simulations per unique combination of vaccination coverage and vaccine immune breadth.

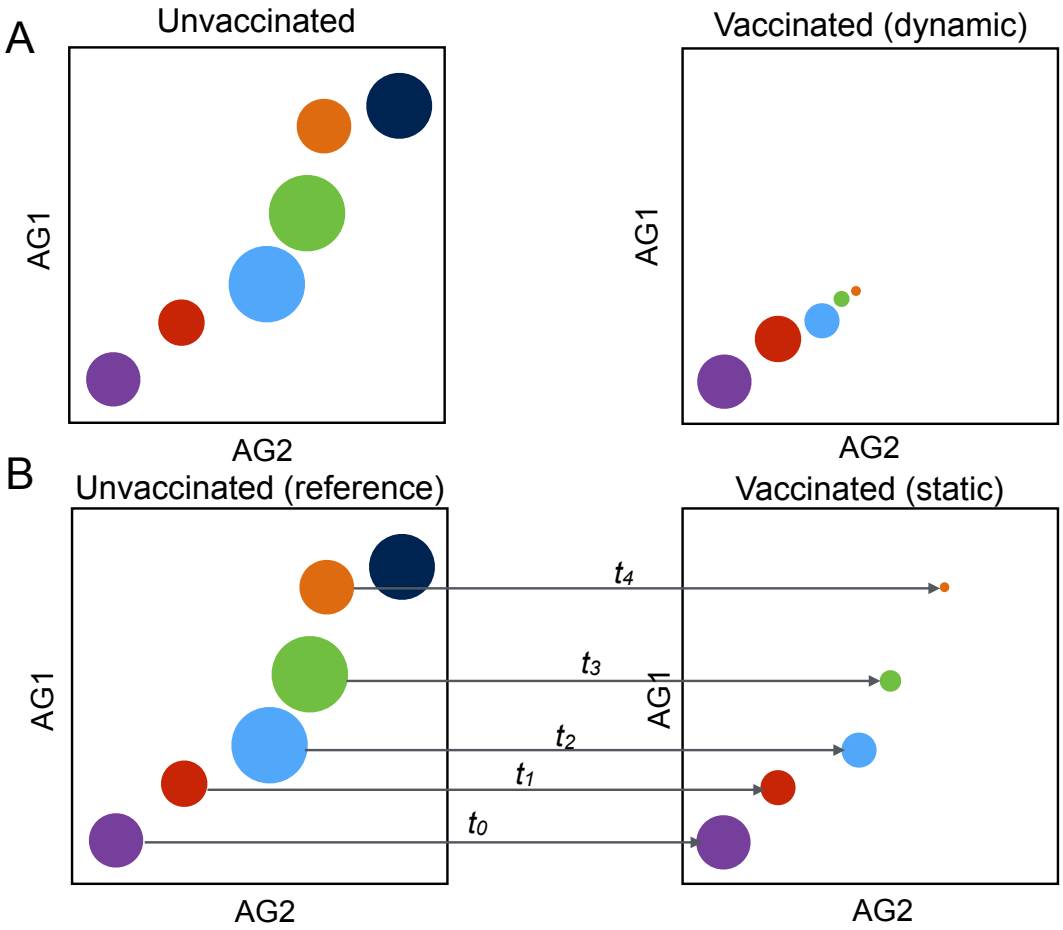

Figure S9: Schematic of the models where vaccination can affect antigenic evolution (dynamic, A) and where vaccination cannot affect antigenic evolution (static, B). Axes represent the principal antigenic dimensions of the 2D antigenic space. The colors of the circles represent the strain phenotypes circulating at a given time interval (the step size of the simulations is one day). The viral population starts in the lower left (purple) and evolves over time to the upper right (dark blue). The size of the circles approximates incidence. (A) In the dynamic simulations, vaccination can affect antigenic evolution. Therefore, the amount of antigenic evolution can decrease and the incidence can decrease relative to no vaccination. (B) In the static simulations, an unvaccinated population is first simulated to generate an evolutionary history that is unaffected by vaccination. Then, in the test simulation with vaccination, the antigenic phenotypes of infections during any time interval are drawn from the unvaccinated reference simulation at the contemporaneous time interval (indicated by the arrows). Thus, the rate of antigenic evolution (the position of the viral population in antigenic space at any time) is independent of vaccination. However, incidence is determined by the epidemiological dynamics of infection and recovery, so vaccination can still affect incidence (indicated by the size of the circles).

Supplemental Material (not copyedited or formatted) for: Frank T. Wen, Anup Malani, Sarah Cobey. 2022. "The Potential Beneficial Effects of Vaccination on Antigenically Evolving Pathogens." The American Naturalist 199(2). DOI: https://doi.org/10.1086/717410.

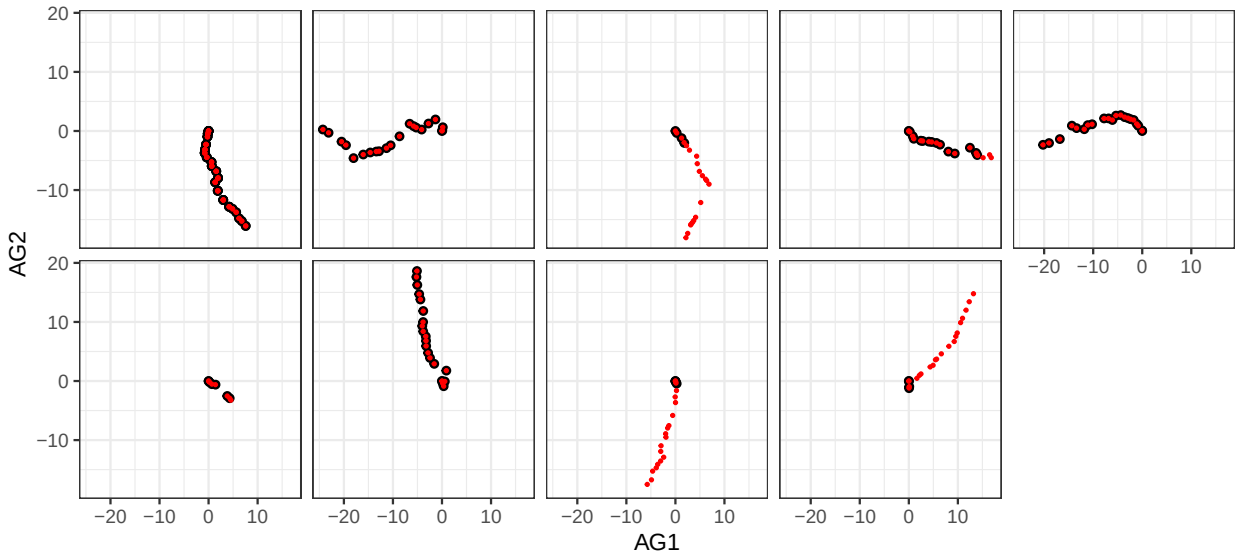

Figure S10: Viral populations in the model where vaccination (i.e. the static model) does not affect antigenic evolution retain the antigenic phenotypes from the reference simulations. Ten random simulations were selected from Figure 3). Each panel shows the trajectory of antigenic evolution in antigenic space for one simulation. Points show the average antigenic phenotype of circulating viruses at the start of each year. Black points show antigenic phenotypes from simulations with vaccination, but where vaccination is not allowed to affect antigenic evolution (i.e. the static simulation). Red points show the antigenic phenotypes from the reference simulation without vaccination used to derive the antigenic phenotypes of the circulating viruses in the corresponding static simulation with vaccination. In cases where red points appear but black points do not, the viral population was driven extinct in the simulation with vaccination, but not in the reference simulation.

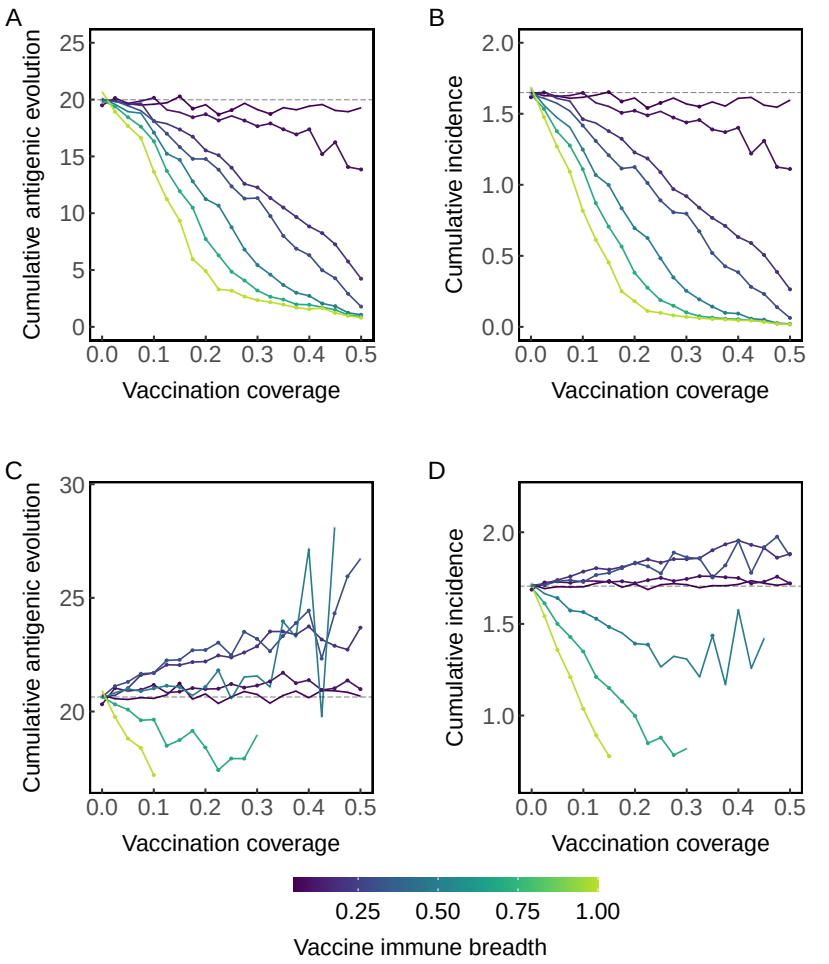

Figure S11: Across all simulations (A&B), vaccination decreases the average (A) cumulative antigenic evolution and (B) incidence regardless of breadth. In the subset of simulations where the viral population does not go extinct (C&D), vaccines with narrow breadth are associated with greater average antigenic evolution (C) and incidence (D), but these increases are not necessarily caused by vaccination (Fig. S14). Lines are colored according to the breadth of vaccine-induced immunity. Points indicate significant decrease (below the dashed line) or increase (above the dashed line) compared to no vaccination according to a Wilcoxon rank-sum test ($p < 0.05$) performed on at least 5 replicate simulations. Complete data are shown in Figures S12 and S15 Data are collected from 500 replicate simulations per unique combination of vaccination coverage and vaccine immune breadth with excessively diverse simulations (TMRCA > 10 years) excluded, leaving $\sim 300 - 400$ simulations per parameter combination.

Supplemental Material (not copyedited or formatted) for: Frank T. Wen, Anup Malani, Sarah Cobey. 2022. "The Potential Beneficial Effects of Vaccination on Antigenically Evolving Pathogens." The American Naturalist 199(2). DOI: https://doi.org/10.1086/717410.

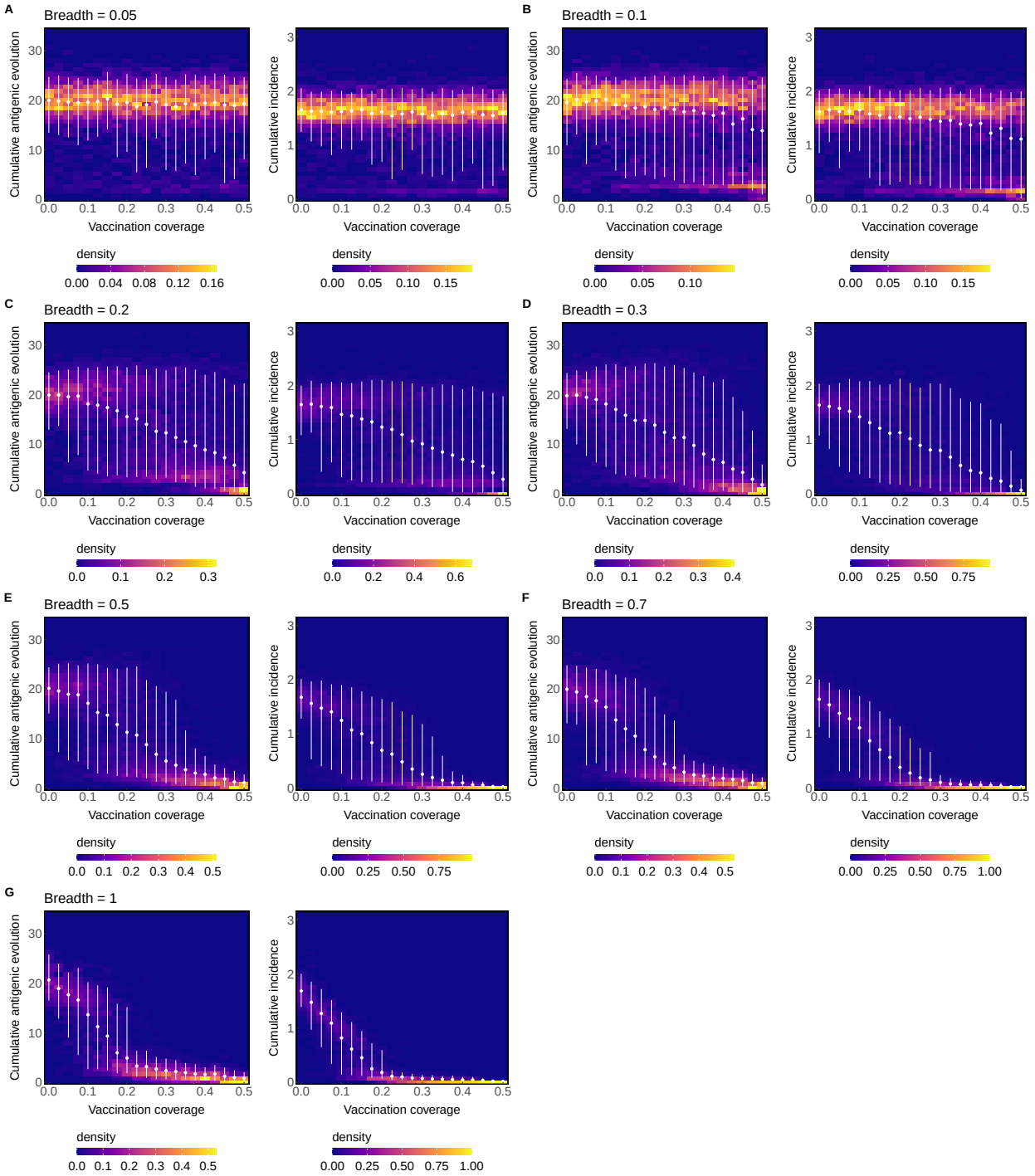

Figure S12: Density plots of complete simulation data corresponding to Figure S11. Points show mean cumulative antigenic evolution or incidence for each vaccination coverage. Error bars show 5th and 95th percentiles for each the simulated outcomes. Data are collected from 500 replicate simulations per unique combination of vaccination coverage and vaccine immune breadth with excessively diverse simulations (TMRCA $>$ 10 years) excluded, leaving $\sim 300 - 400$ simulations per parameter combination.

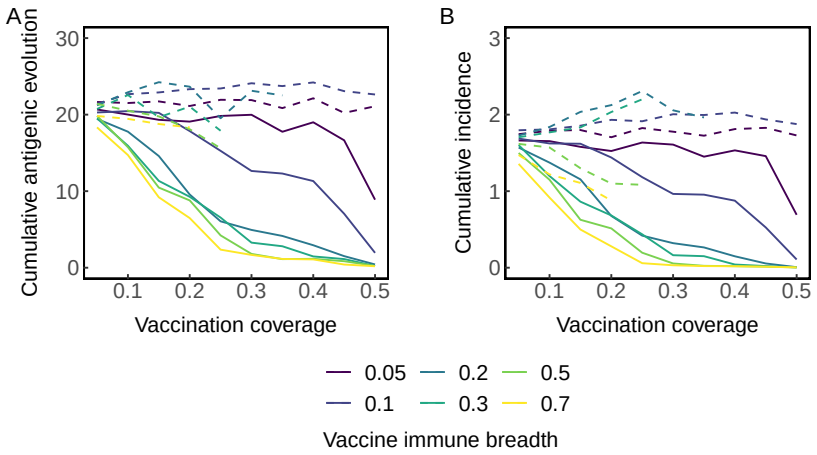

Figure S13: With no temporal lag between vaccine strain selection and distribution, lower vaccination coverage is needed to achieve the same reductions in (A) cumulative antigenic evolution and (B) cumulative incidence compared to when vaccines are distributed 300 days after strain selection (Fig. S11). The solid lines show averages across all simulations, while dotted lines show averages over simulations where the viral population did not go extinct. Lines are colored according to the breadth of vaccine-induced immunity. Data are collected from 200 replicate simulations per unique combination of vaccination coverage and vaccine immune breadth with excessively diverse simulations (TMRCA $>$ 10 years) excluded, leaving $\sim 150 - 160$ simulations per parameter combination.

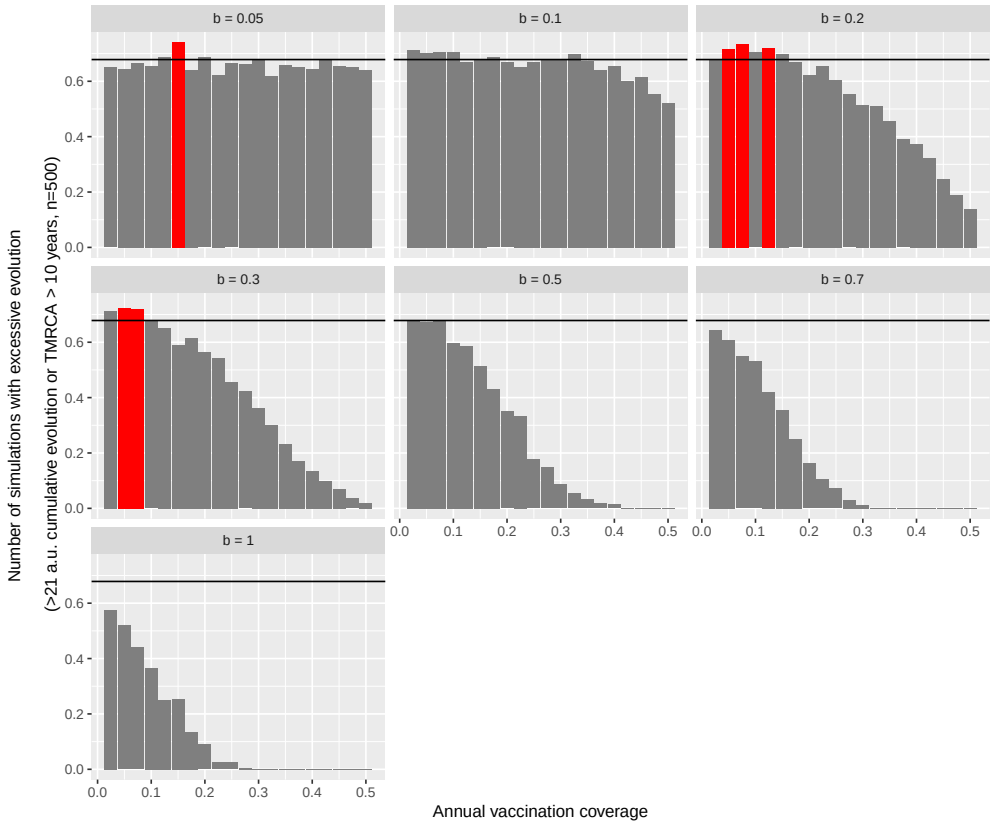

Figure S14: Excessive antigenic evolution with vaccination only occurs at low immune breadth and low vaccination coverage. The subplots show the fraction of simulations (out of 500 replicates for each unique combination of parameters) that demonstrate excessive evolution for each vaccination coverage and breadth b. Here, excessive evolution is defined by either more than 21 antigenic units of cumulative evolution or a TMRCA $>$ 10 years. Black horizontal lines show the number of simulations that evolve excessively without vaccination (the null expectation if vaccines do not drive faster evolution). Red bars show significantly more counts of excessive evolution compared to unvaccinated simulations ($p < 0.05$, Fisher's exact test).

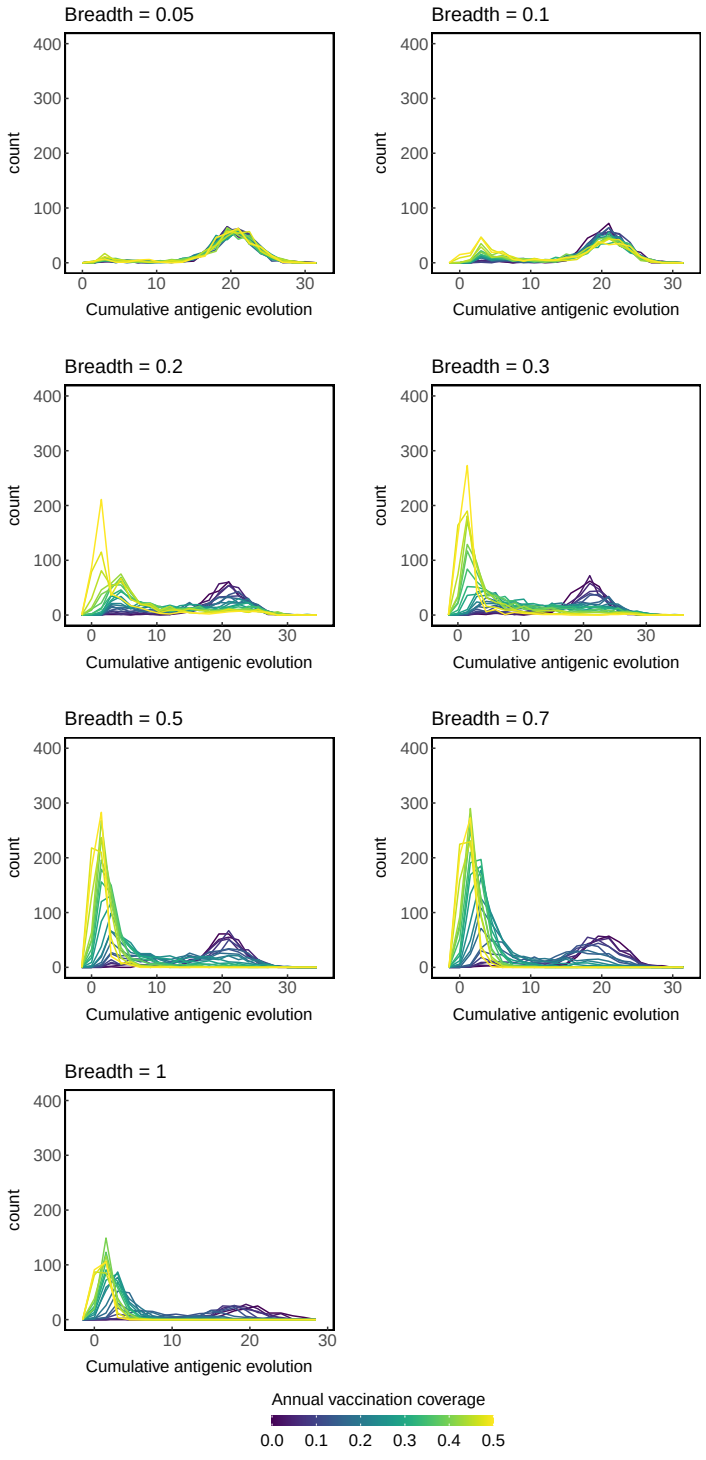

Figure S15: The distributions of cumulative antigenic evolution are profiles along each vaccination coverage shown in figure S12. Data are collected from 500 replicate simulations per unique combination of vaccination coverage and vaccine immune breadth with excessively diverse simulations (TMRCA $>$ 10 years) excluded, leaving $\sim 300 - 400$ simulations per parameter combination.

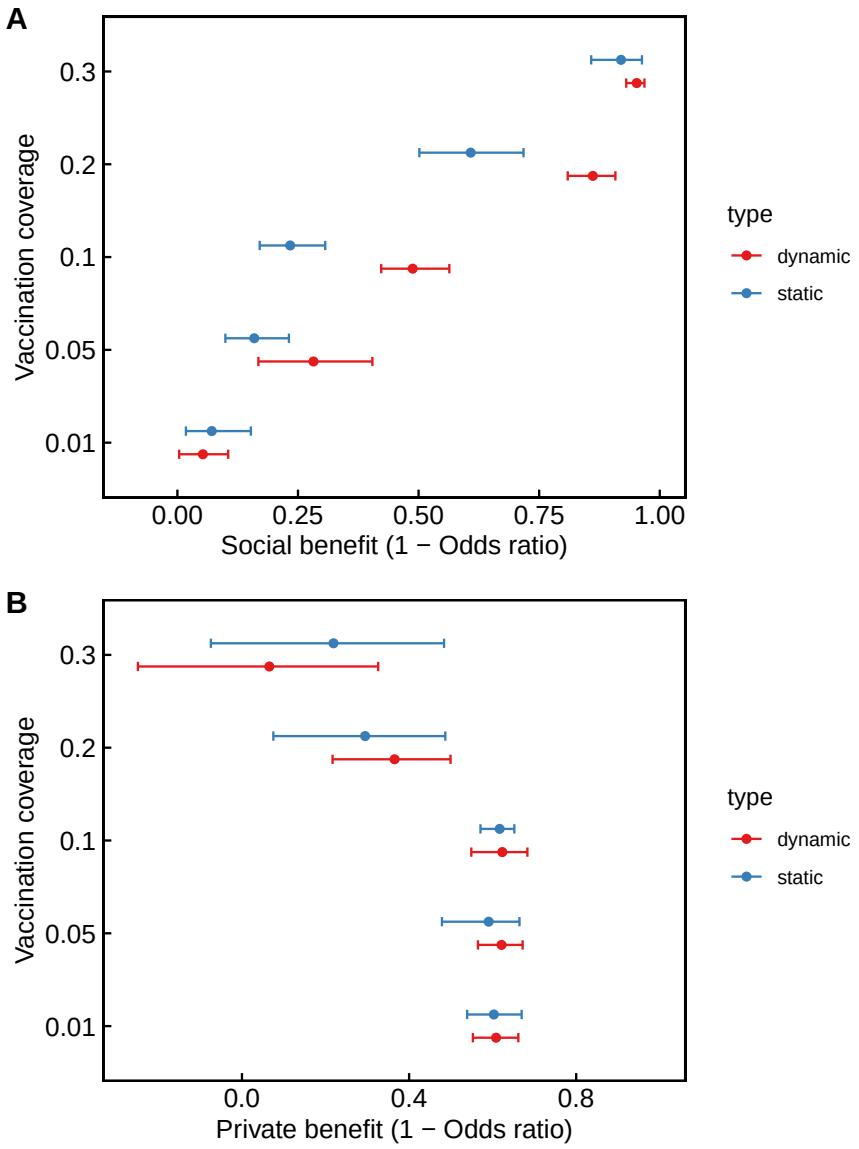

Figure S16: (A) Social and (B) private benefits of vaccination calculated directly from incidence as 1 − Odds ratio (Equations 5 and 7). Effects were calculated from 20 replicate simulations for each vaccination coverage and simulation type using a total of 50,000 individuals for each combination of rate and simulation type. Error bars show bootstrapped 95% confidence intervals. Red lines represent simulations where vaccination can affect antigenic evolution (dynamic). Blue lines represent simulations where vaccination cannot affect antigenic evolution (static).

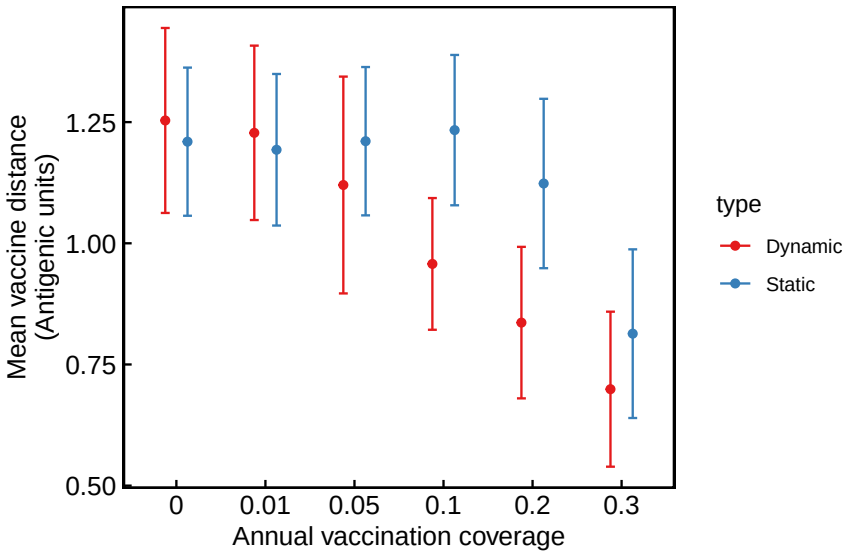

Figure S17: Average distance between the vaccine strain and the average antigenic phenotype of viruses circulating on the first day of the year (for the simulations used to calculate social and private benefits, Figs. 4, S16, Table S3). Distances are calculated using 20 replicate simulations for each unique vaccination coverage and simulation type. Error bars show SDs. Red lines represent simulations where vaccination can affect antigenic evolution (dynamic). Blue lines represent simulations where vaccination cannot affect antigenic evolution (static).

Supplemental Material (not copyedited or formatted) for: Frank T. Wen, Anup Malani, Sarah Cobey. 2022. "The Potential Beneficial Effects of Vaccination on Antigenically Evolving Pathogens." The American Naturalist 199(2). DOI: https://doi.org/10.1086/717410.

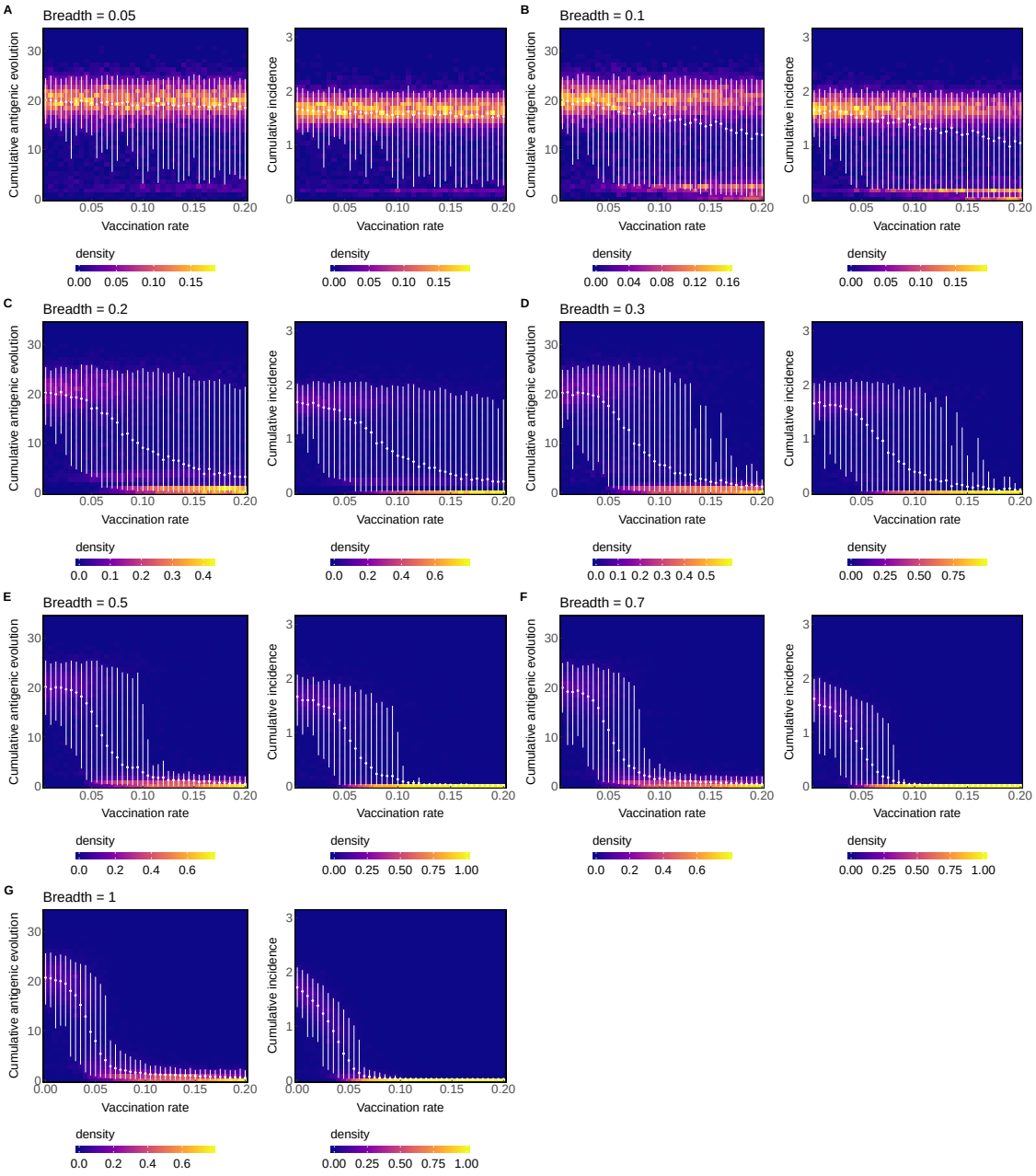

Figure S18: Effects of vaccination on evolution and incidence under a random vaccination strategy. Here, vaccine recipients are randomly selected from the entire population at the beginning of each vaccine season (as opposed to from a preselected pool of candidates). The vaccination rate on the x-axis is the fraction of hosts who are vaccinated each year.

Points show mean cumulative antigenic evolution or incidence for each vaccination rate. Error bars show 5th and 95th percentiles for each the simulated outcomes. Data are collected from 500 replicate simulations per unique combination of vaccination rate and vaccine immune breadth with excessively diverse simulations (TMRCA $>$ 10 years) excluded, leaving $\sim 300 - 400$ simulations per parameter combination.

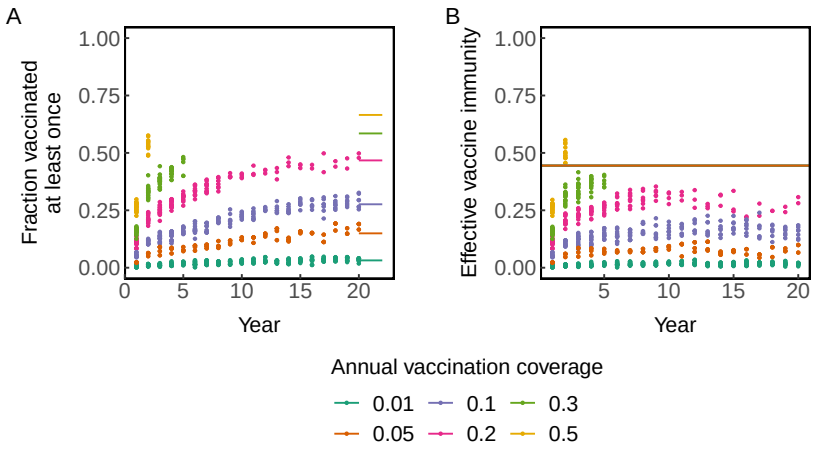

Figure S19: (A) vaccination coverage and (B) effective vaccine-induced immunity over time calculated from simulations. (A) The fraction of individuals who have been vaccinated at least once accumulated over time. (B) The effective amount of vaccine-induced immunity in the population is calculated using the mean antigenic distance between circulating strains and the vaccinated hosts' vaccine strains. At any given time, the effective vaccine immunity is $\frac{1}{N}\sum_i^{Np} \min\{0, 1 - cd_{xv_i}\}$, where N is the host population size, p is the fraction of vaccinated, v_i is the vaccine strain received by individual i, x is the average circulating strain, d is the antigenic distance between the strains, and c is a constant that converts between antigenic distance and risk. Horizontal lines in the right margin of (A) indicate the expected cumulative vaccination coverage after 20 years, determined by a parallel deterministic implementation of the same vaccination strategy. The horizontal line in (B) indicates the theoretical eradication threshold in an antigenically homogenous population $1 - 1/R_0$.

Supplemental Material (not copyedited or formatted) for: Frank T. Wen, Anup Malani, Sarah Cobey. 2022. "The Potential Beneficial Effects of Vaccination on Antigenically Evolving Pathogens." The American Naturalist 199(2). DOI: https://doi.org/10.1086/717410.

Table S3: Private and social benefits of vaccination, reported as absolute risk change from linear regression. In the static model, vaccination cannot affect antigenic evolution. In the dynamic model, vaccination can affect antigenic evolution. Statistics are computed using a linear panel model on longitudinal panel data of simulated hosts' infection and vaccination histories (equation 4). The panel data consist of 50,000 individuals per vaccination coverage with 20 observations per individual. Robust standard errors shown in brackets are clustered by simulation ($^{*}p \leq .05$,$^{**}p \leq .01$,$^{***}p \leq .001$)

	Breadth = 0.5		Breadth = 1	
	Static	Dynamic	Static	Dynamic
Social benefit — 1% vac. rate	1.027	0.991	0.941	0.936
	(1.017 - 1.036)	(0.981 - 1.001)	(0.932 - 0.951)	(0.927 - 0.946)
Social benefit — 5% vac. rate	0.915	0.869	0.854	0.708
	(0.905 - 0.926)	(0.858 - 0.879)	(0.844 - 0.864)	(0.698 - 0.719)
Social benefit — 10% vac. rate	0.788	0.851	0.783	0.509
	(0.777 - 0.799)	(0.84 - 0.861)	(0.772 - 0.793)	(0.499 - 0.52)
Social benefit — 20% vac. rate	0.419	0.308	0.39	0.136
	(0.407 - 0.431)	(0.296 - 0.319)	(0.378 - 0.401)	(0.124 - 0.147)
Social benefit — 30% vac. rate	0.261	0.138	0.078	0.049
	(0.248 - 0.273)	(0.126 - 0.15)	(0.067 - 0.09)	(0.038 - 0.061)
Private benefit (t-0) — 1% vac. rate	0.789	0.736	0.65	0.65
	(0.661 - 0.917)	(0.621 - 0.852)	(0.558 - 0.742)	(0.566 - 0.733)
Private benefit (t-1) — 1% vac. rate	0.796	0.852	0.814	0.813
	(0.629 - 0.964)	(0.706 - 0.999)	(0.691 - 0.938)	(0.699 - 0.928)
Private benefit (t-2) — 1% vac. rate	1.178	1.073	0.93	0.936
	(0.991 - 1.366)	(0.915 - 1.232)	(0.792 - 1.068)	(0.81 - 1.064)
Private benefit (t-3) — 1% vac. rate	0.922	0.988	0.987	0.984
	(0.74 - 1.107)	(0.818 - 1.16)	(0.844 - 1.13)	(0.845 - 1.124)
Private benefit (t-4) — 1% vac. rate	1.126	1.014	0.801	0.886
	(0.972 - 1.281)	(0.87 - 1.16)	(0.69 - 0.912)	(0.774 - 0.999)
Private benefit (t-0) — 5% vac. rate	0.742	0.775	0.607	0.698
	(0.685 - 0.8)	(0.721 - 0.827)	(0.567 - 0.647)	(0.66 - 0.736)
Private benefit (t-1) — 5% vac. rate	0.94	0.929	0.912	0.906
	(0.866 - 1.014)	(0.861 - 0.997)	(0.857 - 0.966)	(0.856 - 0.956)
Private benefit (t-2) — 5% vac. rate	0.995	0.98	0.924	0.96
	(0.916 - 1.073)	(0.905 - 1.054)	(0.864 - 0.985)	(0.906 - 1.015)
Private benefit (t-3) — 5% vac. rate	1.051	1.053	0.89	0.934
	(0.968 - 1.133)	(0.975 - 1.131)	(0.827 - 0.954)	(0.878 - 0.989)
Private benefit (t-4) — 5% vac. rate	1.034	1.034	0.965	0.897
	(0.968 - 1.1)	(0.971 - 1.097)	(0.912 - 1.018)	(0.851 - 0.943)
Private benefit (t-0) — 10% vac. rate	0.854	0.817	0.663	0.78
	(0.814 - 0.894)	(0.778 - 0.857)	(0.634 - 0.692)	(0.756 - 0.803)
Private benefit (t-1) — 10% vac. rate	0.92	0.921	0.877	0.928
	(0.869 - 0.971)	(0.868 - 0.973)	(0.84 - 0.915)	(0.898 - 0.957)
Private benefit (t-2) — 10% vac. rate	0.976	1.015	0.928	0.921
	(0.922 - 1.03)	(0.96 - 1.069)	(0.889 - 0.968)	(0.89 - 0.951)
Private benefit (t-3) — 10% vac. rate	1.022	1.074	0.956	0.978
	(0.966 - 1.078)	(1.018 - 1.13)	(0.913 - 0.998)	(0.945 - 1.01)
Private benefit (t-4) — 10% vac. rate	1.03	0.994	0.924	0.924
	(0.986 - 1.074)	(0.949 - 1.038)	(0.888 - 0.96)	(0.896 - 0.951)
Private benefit (t-0) — 20% vac. rate	1.016	1.084	0.877	0.959
	(0.988 - 1.043)	(1.057 - 1.111)	(0.858 - 0.895)	(0.946 - 0.972)
Private benefit (t-1) — 20% vac. rate	0.991	1.013	0.958	1.004
	(0.957 - 1.025)	(0.982 - 1.044)	(0.934 - 0.982)	(0.988 - 1.019)
Private benefit (t-2) — 20% vac. rate	1.055	1.028	0.962	0.97
	(1.02 - 1.089)	(0.996 - 1.06)	(0.938 - 0.987)	(0.954 - 0.985)
Private benefit (t-3) — 20% vac. rate	0.984	1.025	0.96	0.989
	(0.948 - 1.019)	(0.993 - 1.056)	(0.934 - 0.985)	(0.973 - 1.005)
Private benefit (t-4) — 20% vac. rate	1.079	1.021	0.986	0.967
	(1.049 - 1.109)	(0.996 - 1.046)	(0.964 - 1.007)	(0.953 - 0.98)
Private benefit (t-0) — 30% vac. rate	1.087	1.143	1.003	1.024
	(1.065 - 1.109)	(1.124 - 1.163)	(0.992 - 1.013)	(1.014 - 1.035)
Private benefit (t-1) — 30% vac. rate	1.005	1.019	1.005	0.972
	(0.979 - 1.031)	(0.996 - 1.041)	(0.993 - 1.017)	(0.962 - 0.981)
Private benefit (t-2) — 30% vac. rate	1.022	1.034	0.981	0.986
	(0.996 - 1.049)	(1.012 - 1.056)	(0.969 - 0.992)	(0.98 - 0.993)
Private benefit (t-3) — 30% vac. rate	1.078	1.056	0.986	0.992
	(1.049 - 1.106)	(1.034 - 1.079)	(0.976 - 0.996)	(0.987 - 0.998)
Private benefit (t-4) — 30% vac. rate	1.019	1.055	0.997	0.967
	(0.995 - 1.042)	(1.036 - 1.074)	(0.987 - 1.006)	(0.963 - 0.972)
Constant (baseline odds)	2.137	2.145	2.15	2.155
	(2.136 - 2.138)	(2.144 - 2.146)	(2.149 - 2.152)	(2.154 - 2.156)